Physicochem. Probl. Miner. Process., 61(6), 2025, 214540

http://www.journalssystem.com/ppmp

Physicochemical Problems of Mineral Processing

ISSN 1643-1049

Research on the sedimentation, concentration and strengthening process and mechanism of ultrafine tailings

Hongmei Zhang [1], Yan Wang [1], Fusheng Niu [2], Jinxia Zhang [2], Song Bai [1]

[1] Guizhou Industry Polytechnic College, Guiyang 551400, China

[2] North China University of science and technology, Tangshan 063210, China

Corresponding author: zhanghongmei0316@163.com (Hongmei Zhang)

Abstract: Ultrafine tailing sand was a solid waste generated by the ore dressing process, which seriously affects the efficient large-scale production of mining enterprises due to its fine particle size and slow settling speed. In response to the difficulty of settling and concentration of ultrafine tailings, two kinds of technology for strengthening sedimentation and concentration of tailings were proposed in this paper, namely process strengthening and structure strengthening. In the process strengthening approach, a novel flocculant CF, exhibits optimal sedimentation performance at a concentration of 45% and a dosage of 120 mg/L, achieving a maximum sedimentation velocity of 2.93 mm/s. In the structural enhancement approach, a new deep cone concentrator was designed, which, at a feed rate of 400 mL/min and a scraper rotation speed of 5 rpm, results in a bottom flow concentration of 70.53% after 30 min of sedimentation, demonstrating superior sedimentation concentration performance. The type and content of water in the tailing sand were investigated using Nuclear Magnetic Resonance (NMR), and adsorbed water, pore water and free water were mainly present in the tailing sand, and the active water content in the tailing sand decreased significantly and migrated to more stable water as the settling proceeded.

Keywords: tailings, process strengthening, structural strengthening, strengthening mechanism

1. Introduction

Ultra-fine tailings possess characteristics such as small particle size, high moisture content, and low sedimentation rates. This results in a higher water retention rate in the tailings and a reduced efficiency in dry tailings disposal, significantly impacting the subsequent treatment of the tailings if not addressed with effective processing methods. If the sedimentation rate of solid particles in the tailings was slow, it can result in a significant presence of solid particles and harmful substances in the clarified water, thereby impacting the feasibility of water reuse (Ahmad and Genuchten, 2024; Wen, 2024). At the same time, the slow settling rate of tailings can adversely affect the production efficiency of enterprises, significantly hindering the large-scale operations of mining companies and thereby reducing their profitability (Tang et al., 2023; Deng et al., 2023; Kundu et al., 2023). Therefore, a practical strategy to attain a win-win scenario for both commercial and social benefits is to optimize the settling and concentration processing of tailings using scientifically proven techniques.

Increasing particle size and altering the intricate force field influencing particle sedimentation can improve the settling velocity of particles, according to Stokes' theory of free settling. Consequently, to accelerate the settling rate of tailings, common strategies include the addition of flocculants to encourage the aggregation of fine particles into larger flocs that can precipitate from the liquid, as well as the adjustment of thickener design to facilitate the dewatering of particles being compressed at the base of the thickener cone, subsequently increasing the solid content in the underflow (Que et al., 2022; Guo et al., 2024). Increasing the particle diameter and altering the composite force field of sedimentation are effective strategies for enhancing the settlement velocity of tailings sand (Zhang et al., 2024). To accelerate the sedimentation rate of tailings sand, it was

DOI: 10.37190/ppmp/214540

common to employ the addition of flocculants to modify the particle size, thereby improving the settling velocity of the particles. Han et al. investigated the impact of different flocculants on the settling characteristics of ultrafine tailings, specifically addressing issues such as slow sedimentation rates. The findings indicated that the addition of the anionic flocculant AZ9020 resulted in larger floc sizes with a denser structure and a maximized fractal dimension, enabling rapid sedimentation from the slurry (Han et al., 2022). Li et al. conducted single-factor experiments and response surface methodology to accelerate the sedimentation of ultrafine tailings at SijiaYing. The results showed that when the dosage of flocculant FMC was 215 mL/t, the structure of flocs formed was tighter and stronger, and the flocculant FMC could be effective cost to improve the treatment efficiency of tailings water. The flocculant solution's concentration, the slurry density, and the types and dosages of flocculants all have significant effects on how well tailings settle (Li et al., 2024). Consequently, Peng et al. investigated the flocculation and settling behavior of all-tailings, finding that Flocculant C exhibited the most effective flocculation. The optimal dosage was determined to be 25 g/t, with a flocculant solution concentration of 0.3% and a slurry density of 15%, resulting in the highest settling velocity and maximum treatment capacity per unit area for the tailings. Polyacrylamide has a good effect on flocculation and sedimentation (Peng et al., 2015). Consequently, Gao et al. investigated the flocculation sedimentation characteristics of full tailings under various conditions, including temperature, slurry concentration, type and dosage of flocculants, and the pH of the slurry. The results revealed that a temperature of 25℃, a slurry concentration of 20%, the flocculant being anionic polyacrylamide, a dosage of 20 g/t, and a slurry pH of 6 produced the best results in terms of sedimentation rate and supernatant clarity. Prior to filtration, a thickener was employed to concentrate the concentrate and dewater the tailings. The main purpose of dewatering tailings by thickener was to obtain low turbidity water, so as to realize water recycling and store tailings with low water content in tailings pond (Gao et al., 2019) . In order to optimize process technology operations, it was essential to concentrate the material when the slurry concentration was low, particularly when the operational conditions require a higher concentration (Landman et al., 1988). As a result, one of the most important pieces of dewatering machinery in the manufacturing of mineral processing was the thickener. To address the issue of low tailings discharge concentration and large particle size in mineral processing plants, Yao et al. conducted a study on tailings discharge and concentration techniques. The results indicated that after employing classification machines to separate some of the larger particles from the tailings, concentration equipment could elevate the tailings discharge concentration to over 35%. This approach not only reduced the transportation costs associated with tailings but also extended the operational lifespan of tailings storage facilities, thereby enhancing their safety factor (Yao et al., 2023). Zhang et al. employed a non-ionic flocculant with a molecular weight of 12×106 to enhance the sedimentation and concentration of tailings within a thickener. The findings demonstrated that the flocculant's settling rate was proportional to its dosage, thereby resulting in an underflow concentration that peaked at 40 g/t (Zhang et al., 2023). The application of thickening machines contributes significantly to the enhancement of tailings sedimentation performance. Tan conducted laboratory deep cone thickening experiments, revealed that a higher fine particle content in the tailings correlates with a slower sedimentation efficiency (Tan, 2020). Flocculants can aggregate fine particles into larger flocs, facilitated their rapid settling from the slurry. Furthermore, when the feed concentration reached 25%, the maximum underflow concentration can be achieved (Liu et al., 2022). Current research primarily focuses on the types, dosage, and feed concentration of flocculants in relation to the sedimentation performance of tailings. However, there is limited investigation into the synthesis of novel agents and the enhancement of sedimentation and concentration processes through innovative equipment.

This study synthesizes novel flocculants and conducts experiments on the concentration and dosage of these flocculants to enhance the sedimentation of ultra-fine tailings. Based on the characteristics of the ultra-fine tailings, a new type of deep cone concentrator was designed to investigate the impact of its structure on sedimentation and concentration performance. Based on the difference of water locking capacity of floc network structure, the migration and transformation behavior of water in tailing sand was investigated, and two mechanisms to strengthen the performance of ultrafine tailing sand settlement and concentration were carried out, so as to provide theoretical basis for ultrafine tailing

sand settlement and concentration.

2. Materials and methods

2.1. Materials

2.1.1. Particle size composition

The test sample was made up of ultrafine tailings from a Hebei mineral processing facility. The particle size distribution of the sample was analyzed using a Mastersizer 2000 laser particle size analyzer. The particle size of the tailings was determined by the volume-weighted average particle size method， and the results are presented in Fig. 1.

Based on Fig. 1, it was evident that the tailing sand samples contain more fine-grained grades, with a content of 38.93% for particles -10 μm, 57.86% for those -20 μm, and a mere 0.8% for particles +100 μm. The D50 of the sample was determined to be 16.63 μm, and the mean particle size was calculated at 25.00 μm, indicating that the sample consisted of fine particles, classifying it as ultrafine tailings.

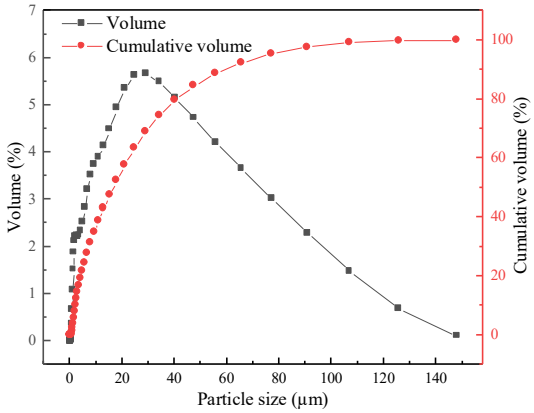

Fig. 1. Particle size distribution of ultrafine iron tailings

2.1.2. Chemical multielement

The settling, concentration, and dewatering properties of the tailings slurry were all significantly influenced by the chemical makeup of the ultrafine tailings. The test samples were reduced for sampling, and three representative samples were taken and tested using a ZSX Primus II X-ray fluorescence spectrometer, and the difference of detection results was small. The average value of the three sets of data was calculated for the multi-element chemical analysis of fine-grained iron tailings, with results presented in Table 1.

Table 1. Chemical element analysis of overflow superfine tailings %

SiO_2	Fe_2O_3	CaO	Al_2O_3	MgO	K_2O	Na_2O	TiO_2	P_2O_5	SO_3	MnO	ZnO
60.13	14.21	9.14	7.21	3.88	2.45	1.12	0.63	0.6	0.47	0.12	0.04

The main constituents of the ultrafine tailings were SiO_2, Fe_2O_3, CaO, and Al_2O_3, as shown in Table 1. SiO_2 was the most prevalent at 60.13%, followed by Fe_2O_3 at 14.21%, and a number of oxides were detected at concentrations lower than 5%.

2.1.3. Mineral composition

The mineral composition of the tailings was analyzed using a D/MAX2500PC X-ray diffractometer. The test parameters were set to 40 kV and 100 mA, with a scanning range of 10° to 80°, a step size of 0.02°, and a scanning speed of 10° per minute. The results of the X-ray diffraction (XRD) analysis are presented in Fig. 2 Minerals include Quartz, Anorthite, Montmorillonite, Kaolinite, Chlorite, Hematite, Amphibole, and Magnetite were the principal constituents of the tailings samples. Quartz hasd the highest concentration of them, included clay minerals such Montmorillonite and Kaolinite. These elements impaired tailings sedimentation performance.

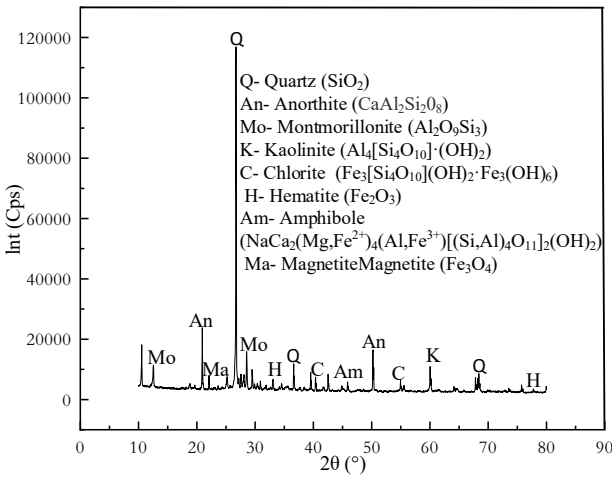

Fig. 2. XRD analysis of overflow superfine tailings

2.2. Flocculant preparation

The ferric trichloride solution derived from the industrial waste acid cleaning fluid was amalgamated with the industrial polymeric aluminium chloride in a proportion of 1:4 and introduced into a beaker. Deionized water was successively incorporated and agitated until complete dissolution. The experimental temperature was scrupulously regulated using a constant-temperature water bath, enabling the polymerization process to ensue at a maturation temperature of 40 ℃ for 8h until the reaction reached its conclusion. To create the flocculant, the resulting polymerized product was then uniformly mixed after being allowed to naturally cool to ambient temperature, and this flocculant was named CF flocculant. XRD analysis of CF flocculant showed that the main phase compositions in the flocculant CF were $(Fe_{0.86}Al_{0.14})2O_3$, $AlCl_3{\cdot}2Al(OH)_3!6H_2O$, $Al_{13}Cl_{15}(OH)_{24}!37.5H_2O$, $Al_5Cl_3(OH)_{12}!7.5H_2O$, $Al_2Fe_2O_6$, and $Fe_3(S0_4)_2(OH)_3!2H_2O$. Numerous unknown peaks appear in the product, indicating that it is complex and amorphous.

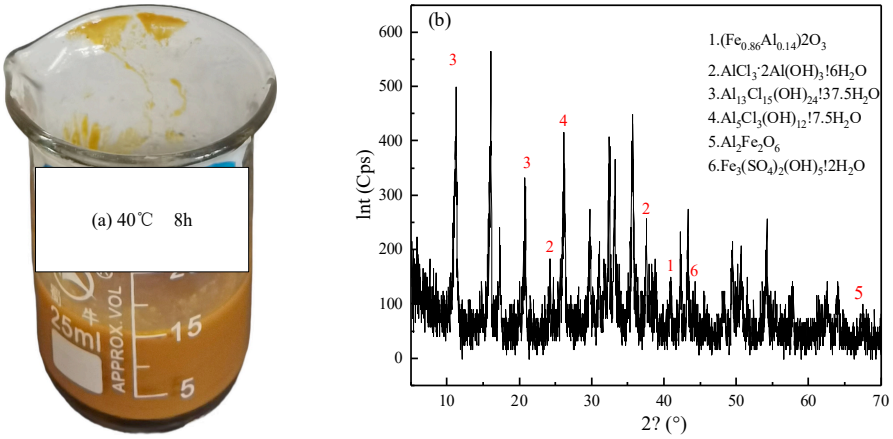

Fig. 2. Flocculant CF: (a) flocculant CF picture; (b) XRD of flocculant CF

2.3. Design of new deep cone thickener

Utilized the principle of gravitational settling, solid particulates were compelled to descend due to gravitational forces, whereas the clarified liquid phase ascended towards the surface. Specifically designed to address the granular distribution, slurry characteristics, and sedimentation properties of ultrafine tailings, the novel deep-cone thickener increased the tailings' vertical settling duration and optimized the slurry's residence time on the inclined plane. This was achieved by strategically adjusting the inclination angle and the height of the thickening chamber, which in turn, markedly improved the concentration of the underflow. The schematic representation of the novel deep-cone thickener was illustrated in Fig. 3, with its crucial parameters detailed in Table 2.

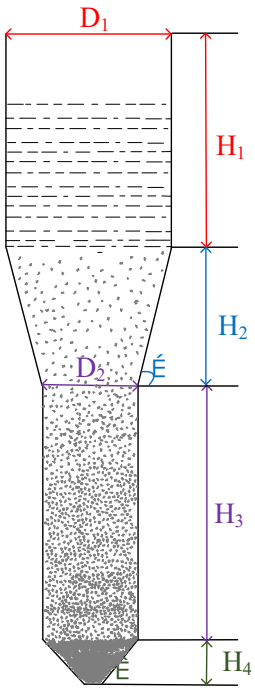

Fig. 3. New Deep Cone Thickener

Table 2. Main parameters of new deep cone thickener

Name	D_1/mm	D_2/mm	H_1/mm	H_2/mm	H_3/mm	H_4/mm	α/°	β/°
Parameter	120	80	130	100	160	30	40	60

2.4. Test method

The structure-enhanced sedimentation test, designed to simulate the dynamic flocculation process subsequent to the entry of tailings into the concentrator and their interaction with flocculants was utilized. Solid concentration within the clarified, interference, and compression zones was employed as metrics for evaluation. In the experiment, the concentration of flocculant CF was determined to be 45% by static flocculation and sedimentation test, with a slurry concentration of 4.5%, which was used to establish the best parameters of sedimentation and concentration.

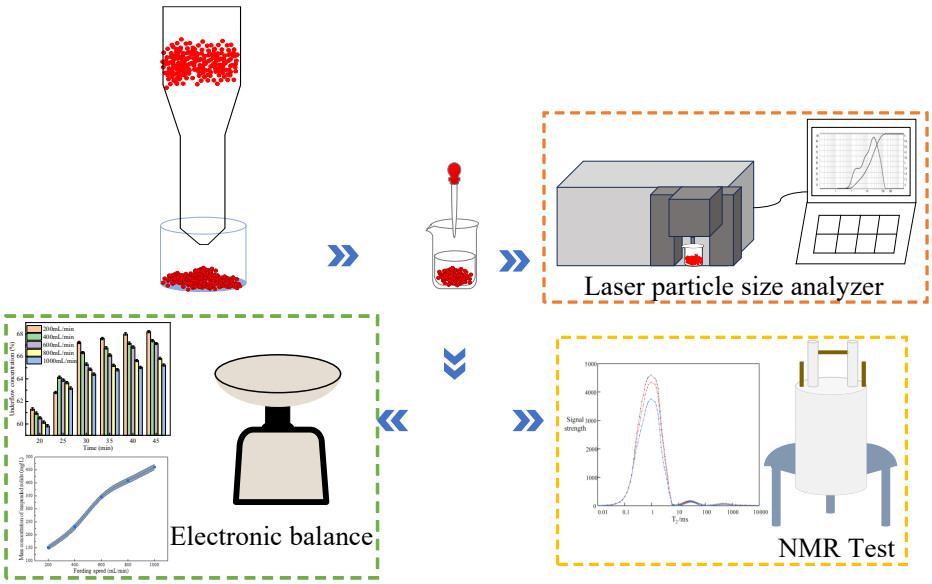

Fig. 4. Structure strengthening settlement test device diagram

3. Results and discussion

3.1 Dynamic characteristics of process-enhanced settlement

3.1.1. Effect of flocculant concentration on sedimentation and concentration of ultrafine iron tailings

The optimal sedimentation effect of the flocculant on ultrafine iron tailings was identified, leading to an investigation of the sedimentation performance of ultrafine iron tailings at flocculant CF concentrations ranging from 20% to 50%. The study aimed to determine the impact of varying concentrations of flocculant CF on the sedimentation characteristics of ultrafine iron tailings, with the findings being crucial for establishing the most effective flocculation and thickening parameters.

The settling velocity of ultrafine iron tailings sand progressively increased as the flocculant CF concentration rised, as seen in Fig. 6. The settling velocity at the initial settling moment progressively rised from 1.4 mm/s at 20% concentration to 2.25 mm/s at 45% concentration. When flocculant CF concentration reached 50%, the settling velocity dropped from 2.25 mm/s to 2.13 mm/s. The greatest settlement velocity was 2.78 mm/s during the settlement process when the settlement period was 90 s. It was discerned that the settling velocity precipitously increased at the onset of the sedimentation process, subsequently declined gradually, and ultimately stabilized after approximately 300 s. Further analysis revealed that at a CF concentration of 45%, the maximum sedimentation velocity was recorded at 2.78 mm/s. This discovery confirmed that the ideal concentration of flocculant CF was kept at 45%, so that ultrafine tailings had the best flocculation and sedimentation performance.

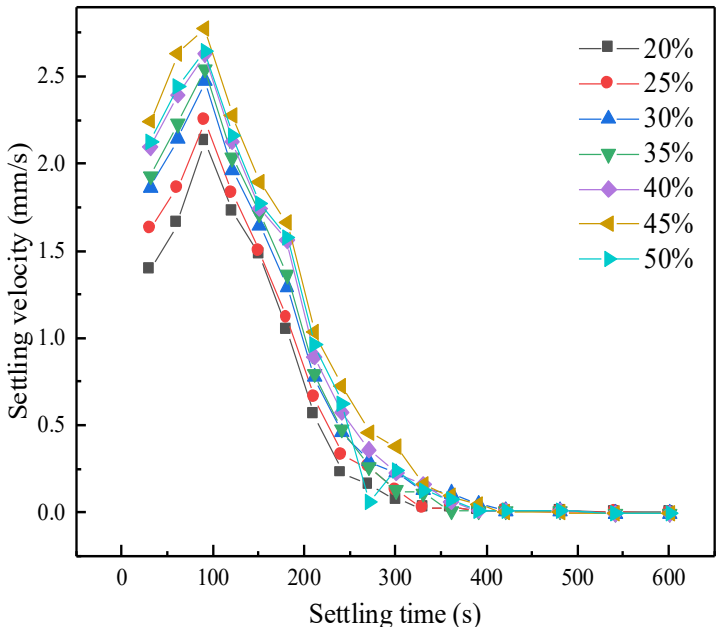

Fig. 6. Effect of CF concentration on settling velocity of tailings

3.1.2. Effect of flocculant dosage on sedimentation and concentration of ultrafine iron tailings

The sedimentation performance of ultrafine iron tailings was investigated at a flocculant CF concentration of 45%, with dosages ranging from 30 to 180 mg/L. The results were depicted in Fig. 7.

The settling velocity of tailings sand particles increased during the settling procedure and then reduced when the flocculant CF dosage raise, as displayed in Fig. 7. When flocculant CF dosage was less than 120 mg/L, the settling speed of ultrafine tailings increased as flocculant CF dosage increased at the same settling time. At a starting concentration of 30 mg/L, the settling velocity progressively rosed from 0.8 mm/s to 2.47 mm/s. After reaching its maximum value of 2.93 mm/s at a settling duration of 90 s, the settling velocity progressively declined. When the flocculant CF dosage was higher than 120 mg/L, the settling speed fell as the flocculant CF dosage increased. At a starting concentration of 120 mg/L, the settling velocity progressively dropped from 2.47 mm/s to 1.57 mm/s. The settling velocity steadily dropped from 2.93 mm/s at 120 mg/L to 2.1 mm/s after 90 s of settling. This phenomenon was attributed to the fact that at dosages surpassing 120 mg/L, the flocculant CF caused

an overabundance of Fe^{3+} and Al^{3+} to be released, leading to a reversal of the slurry's ζ potential to a positive value due to the predominant presence of cations. The flocculation efficiency and the settling velocity consequently decreased as a result of the positively charged mineral particles' repulsive interactions with the flocculant's Fe^{3+} and Al^{3+} ions, which ultimately resulted in the formation of smaller flocs or fewer aggregates. The data presented led to the conclusion that the sedimentation velocity reached a maximum of 2.93 mm/s at a flocculant CF dosage of 120 mg/L. Considering sedimentation velocity and turbidity, the optimal concentration of flocculant CF was determined to be 45%, where the flocculation and sedimentation effect on ultra-fine tailings was most efficacious.

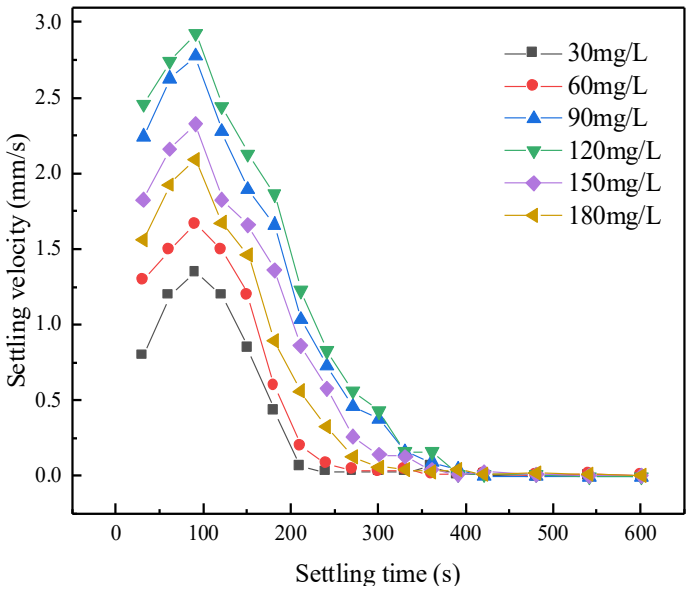

. 7. Effect of CF dosage on settling velocity of tailings

3.2 Dynamic characteristics of reinforced settlement of structure

3.2.1. Influence of thickener structure on sedimentation and concentration effect of ultrafine iron tailings

The settling performance of the tailings was found to vary across different sedimentation zones. An analysis of the solid concentrations within the settling zone, interference zone, and concentration zone of a novel deep cone thickener revealed significant differences in concentrations across these distinct sedimentation areas, as depicted in Fig.8.

The solid concentration in the setting zone rapidly decreased from 18.07% at 2 min to gradually flattening out as the settling time increased, depicted in Fig. 8. After settling for 40 min, the solid concentration was 0.005%. After 2 min, the solid concentration in the interference zone dropped from 27.68% to 0.42%, and after 40 min of settling, it was just 0.01%. The solid concentration in the concentration zone rised dramatically, from 17.20% at 2 min to 63.34% in a short period of time, in contrast to the setting zone and interference zone. The solid concentration in the concentration zone varies less when the settling time was longer than 30 min.

At the commencement of sedimentation, that is, at the 2 min mark, the interference zone was found to harbor the highest solid concentration, succeeded by the setting zone, while the concentration zone registered the lowest. Throughout the sedimentation process, the solid concentration in the interference zone consistently exceeded that of the setting zone, suggested that the interference zone plays a pivotal role in the aggregation of sedimenting particles. This was attributed to particles transitioning from the setting zone and residing within the interference zone, consequently elevating its solid concentration. After a sedimentation period of 40 min, the concentration zone was observed to exhibit the highest solid concentration, followed by the interference zone and then the setting zone. Furthermore, it was clear that during the sedimentation process, the concentration zone's solid concentration stayed higher than the interference zone's. This was indicative of particles aggregating and settling in the concentration zone subsequent to their passage through the interference zone, culminating in a heightened solid concentration within the concentration zone.

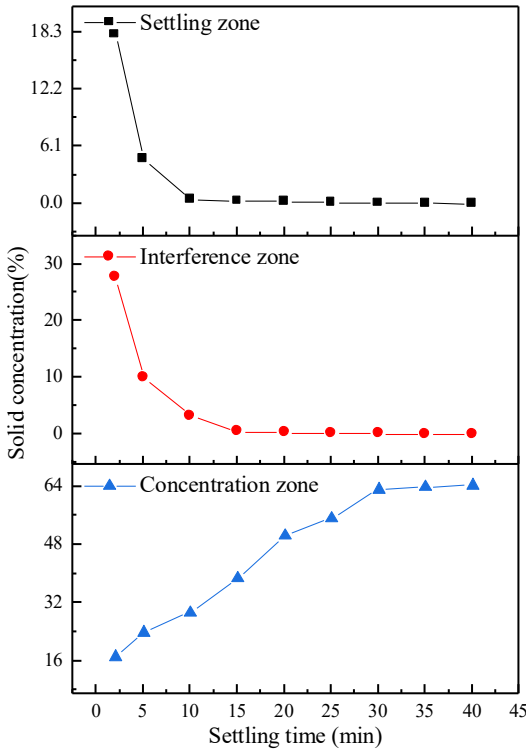

. 8. Solids concentration in different settlement regions

3.2.2. Effect of feeding speed on sedimentation and concentration of ultrafine iron tailings

The sedimentation concentration of ultrafine iron tailings sand was shown to be considerably influenced by the slurry's feed rate. The effect of different feed rates on the mass concentration of suspended solids in the overflow and the bottom flow concentration was thus investigated. Tests monitoring the sedimentation concentration were performed at feed rates of 200 mL/min, 400 mL/min, 600 mL/min, 800 mL/min, and 1000 mL/min, with the bottom flow concentration findings demonstrated in Fig.9.

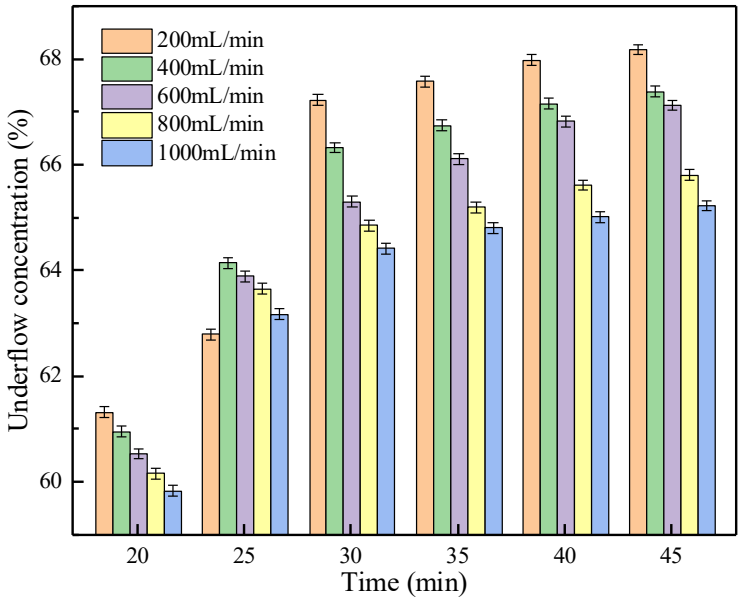

Fig. 9. Effect of feeding speed on underflow concentration

The bottom flow concentration of ultrafine iron tailings sand was observed to increment gradually with the elongation of sedimentation time, as illustrated in Fig. 9. A significant rise in concentration was noted during the interval from 20 to 30 min of sedimentation, with scant variation occurring subsequent

to 30 min. After 20 min of settling, the bottom flow concentration quickly rised from 61.34% to 68.2% at a feed rate of 200 mL/min. At a feed rate of 400 mL/min, the underflow concentration was observed to increased from 60.97% to 67.41%. When the feed rate was elevated to 600 mL/min, the underflow concentration increased from 60.55% to 67.15%. At a higher feed rate of 800 mL/min, the underflow concentration augmented from 60.18% to 65.83%. Ultimately, at the maximum feed rate of 1000 mL/min, the underflow concentration was tracked to shift from 59.85% to 65.25%. Therefore, it was clear that when the feed rate increased, the underflow concentration generally tended to decrease, achieving its peak of 67.25% at a feed rate of 200 mL/min and after 30 min of sedimentation.

3.2.3. Effect of scraper speed on sedimentation and concentration of ultrafine iron tailings

The scraper speed of the concentrator was identified to influence the mixing efficiency of tailings sand with the flocculant, consequently affecting the sedimentation concentration of fine iron tailings sand. As a result, an analysis was conducted to determine how scraper speed affected the concentration of suspended materials in the overflow as well as the concentration in the underflow. Experiments pertaining to sedimentation concentration with tailings sand were conducted at scraper speeds of 0 rpm, 2 rpm, 5 rpm, 8 rpm, and 10 rpm. The outcomes pertaining to underflow concentration were depicted in Fig. 10.

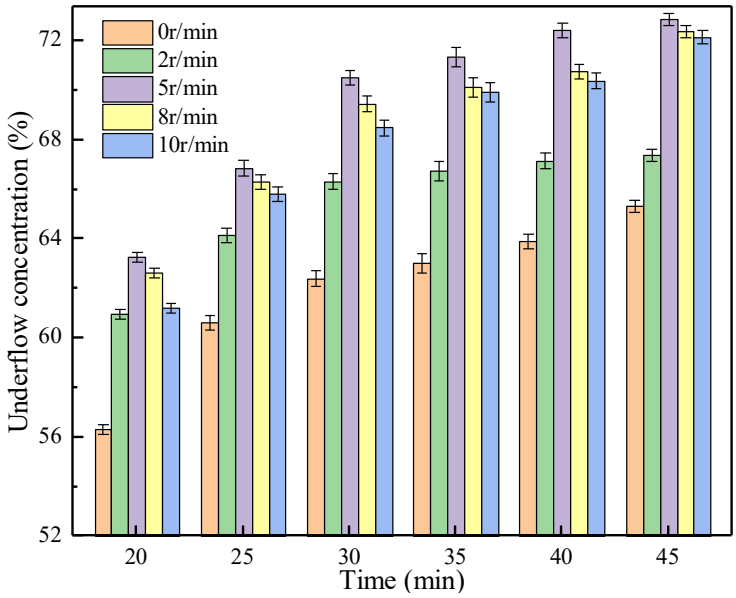

Fig. 10. Influence of scraper speed on underflow concentration

As depicted in Fig. 10, when the scraper rotating speed was set at 0 rpm, the underflow concentration was observed to increased from 56.34% to 65.35%. At a scraper speed of 2 rpm, the underflow concentration was found to elevate from 60.97% to 67.41%. At a scraper speed of 5 rpm, the underflow concentration demonstrated a significant increase from 63.27% to 72.91%. At 8 rpm, the underflow concentration rose from 62.65% to 72.42%. Upon raising the scraper speed to 10 rpm, the underflow concentration was noted to expand from 61.25% to 72.18%. Hence, it was observed that the underflow concentration generally increased initially with the increment of scraper speed and subsequently decreased. The maximum underflow concentration was achieved at a scraper speed of 5 rpm, reaching 70.53% after 30 min of sedimentation.

3.3 Water migration and transformation behavior of tailings

3.3.1. Moisture types in tailings

Free water and bound water were the two types of moisture that were present inside the floc structure as the tailings particles settled and then gathered to form the floc structure. Depending on the types of moisture present inside the flocs, the moisture in the tailings was further separated into four distinct groups in this article.

① **Free water**: This sort of moisture, often referred to as interstitial water, was characterized by the absence of interaction forces with tailings particles or flocs. It could be separated from solids by intermittent sedimentation.

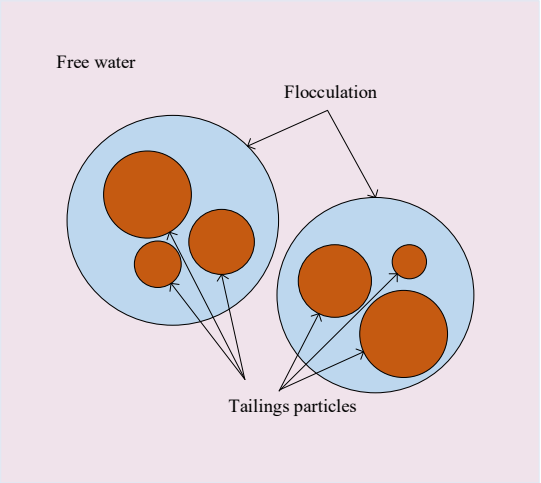

Fig. 11. Distribution of floc free water

② **Pore water**: A critical component of bound water, was discovered within the floc structure's voids. When exposed to gravitational or shear pressures, the floc structure's integrity was disrupted, allowing pore water to be released.

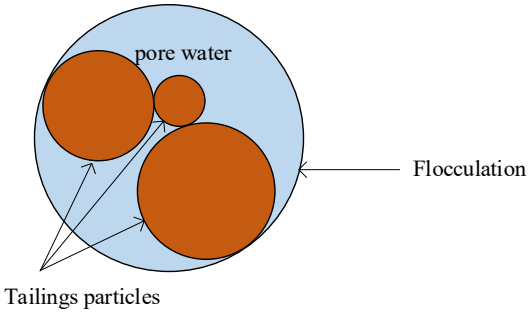

Fig. 12 Pore Water Distribution of Floccules

③ **Adsorbed water**: This moisture was found to be present on the surface of the tailings particles, where it adhered or adsorbs. It also showed a strong surface interaction with the tailings. The tailings of metal ore, which frequently had a small number of ultrafine particles smaller than 20μm, had a large surface area and were colloidal in the slurry, which allowed for "self-flocculation" and resulted in a significant amount of surface water becoming adsorbent. It was commonly noted that the removal of surface water with gravitational thickening techniques was challenging.

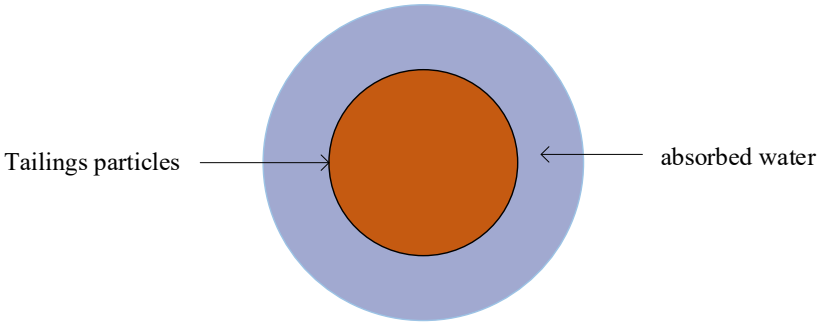

Fig. 13. Distribution of flocs adsorbed water

④ **Combined water**: This kind of moisture was produced when solid particle surfaces interacted with chemical bonds. To liberate the bound water, methods like thermal chemical degradation were usually needed.

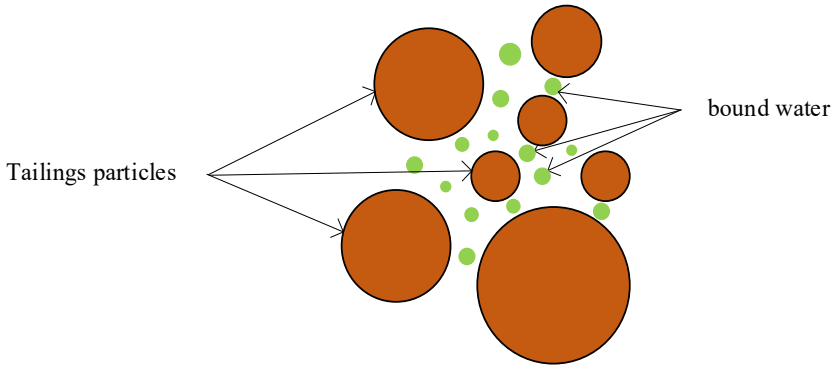

Fig. 14. Distribution of flocs bound water

It demonstrated how the sedimentation and flocculation processes raised the level of flocculation between the tailings particles, which eventually led to the formation of flocs. When the quantity of flocs rose, their better adsorptive bridging resulted in the formation of a floc structure in the sediment layer. Due to the retention of pore water in the interior gaps and interstitial water in the spaces between the flocs, respectively, a direct connection between the moisture within the flocs and their structure was established.

3.3.2. Effect of flocculant on water migration during tailings sedimentation

It was possible to investigate the moisture migration patterns of the tailings during sedimentation at intervals of 1, 5, and 10 min by using nuclear magnetic resonance to detect the transverse relaxation time T_2 distribution of water in the tailings, both with and without the addition of flocculants. The findings of this study were exhibited in Fig. 15.

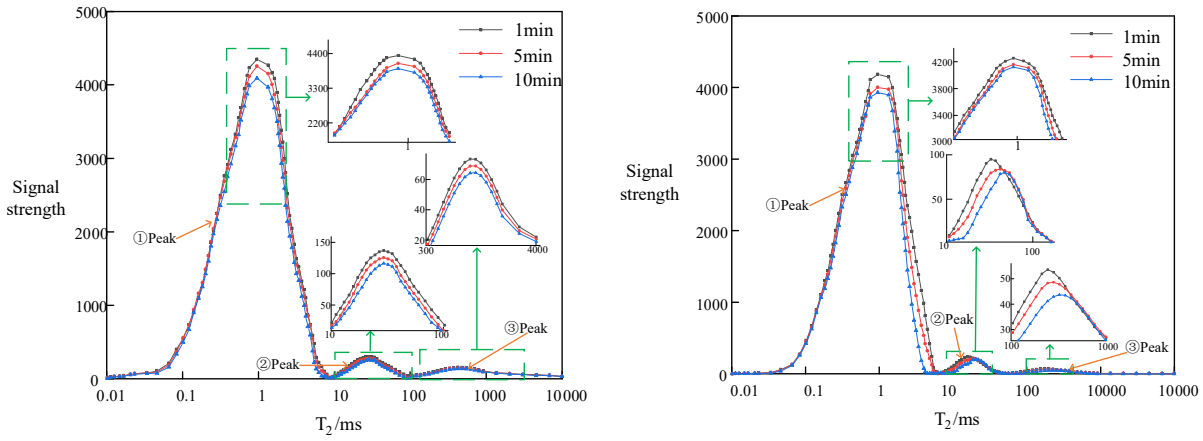

Fig. 15. Distribution of water T_2 spectra with and without CF at different sedimentation times

Fig. 15 showed that regardless of the addition of the flocculant CF, the tailings sand had three unique relaxation peaks at different sedimentation times. Peaks ①, ②, and ③ represented distinct water states, corresponded to different states of water. When the T_2 value was less than 1 ms, the water was classed as adsorbed water; when it was between 1 and 100 ms, it was classified as pore water; and when it exceeded 100 ms, it was defined as free water. A lower T_2 value showed a smaller degree of freedom for the water molecules, meaning tighter environmental limitations and decreased mobility. As a result, the three peaks in the T_2 spectrum were identified as adsorbed water, pore water, and free water, with the integral values of the curves reflecting the peak areas. Variations in peak area indicated the migration

and transformation of adsorbed, pore, and free water within the tailings sand. And indicated that in both the presence and absence of the flocculant CF, the areas of the three relaxation peaks reduced with increasing sedimentation time, indicating a decrease in the content of each water type. This implied that as time passed, the active moisture inside the tailings sand shifted toward a more stable form. Fig. 15(a) showed that when no flocculant CF was applied, Peak ① had the biggest area, indicating that adsorbed water was the dominant type during sedimentation, followed by pore water, and free water was the least prevalent. The settling process, which lasted from 1 to 5 and 10 min, resulted in a reduction of the adsorbed water, pore water, and free water. This was because the hydration reaction, which took place after the tailings sand particles came into contact with water, changed the non-chemically bound water into chemically bound water. Since this was not detectable by NMR, the quantity of the water could not be quantitatively described. Fig. 15(b) showed that adding flocculant CF did not significantly change the peak area of peak ①, indicating that the tailings sand was still dominated by adsorbed water during the settlement process. The area of peak ② and peak ③ also decreased, and as the settling time increased, the area of peak ② and peak ③ decreased more significantly, indicating a decrease in the content of pore water and free water in the floc structure in tailings sand. Following the addition of the flocculant CF, Fig. 15 showed that the amounts of free water and pore water in the tailings sand changed. This helped to facilitate the movement and transformation of the free water and pore water in the tailings. When the flocculant CF was not applied, the tailings sand particles mostly produce flocs via "self-flocculation," and the floc net formed by this "self-flocculation" had poor water locking properties. After adding the flocculant CF, the electric double layer and adsorption bridging allowed tailings sand particles to form flocs with larger particle sizes and more compact structures, increasing the conversion of free water into more stable pore water in flocs.

Table 3. Relaxation peak area of tailings T_2 spectrum with and without CF

Time/min	① Peak		② Peak		③ Peak	
	without CF	with CF	without CF	with CF	without CF	with CF
1	37.65	34.56	1.36	1.23	0.64	0.54
5	34.72	31.43	1.12	1.06	0.53	0.42
10	33.29	30.58	0.97	0.87	0.39	0.28

As demonstrated in Table 3, the peak area of the tailings sand ① peak without flocculant CF decreased from 37.65 to 34.72 and 33.29, indicating a drop of 7.78% and 4.12%, respectively. The peak area of ② peak reduced from 1.36 to 1.12 and 0.97, with a decrease of 17.65% and 13.39%, respectively. The peak area of ③ peak decreased from 0.64 to 0.53 and 0.39, with decrease rates of 17.18% and 26.42%. The peak area of the ① peak of tailings sand treated with flocculant CF dropped from 34.56 to 31.43 and 30.58, respectively, with decrease rates of 9.06% and 2.70%. The ② peak area declined from 1.23 to 1.06 and 0.87, respectively, by 13.82% and 17.92%. The ③ peak area decreased from 0.54 to 0.42 and 0.28, respectively, by 22.22% and 33.33%. The overall water content of tailings reduced from 34.65% without flocculant CF to 31.73% after 10 min of settling, representing an 8.43% decrease.

3.3.3. Effect of thickener structure on water migration during tailings settlement

The water movement law of tailings in the clarifying zone, interference zone, and concentration zone when settled in thickener was investigated. Fig. 16 depicted the distribution of water in tailings with transverse relaxation time T_2.

It can be seen from Fig. 16 that there were three relaxation peaks in the three settling areas of setting zone, interference zone and concentration zone at different settling times. Adsorbed water, pore water, and free water were represented by the three peaks, which ran from left to right. The peak area is shown by the curve's integral value, and the migration and transformation of adsorbed, pore, and free water in tailings was represented by the change in peak area. Fig. 16 showed that the three relaxation peak areas of tailings in setting zone, interference zone, and concentration zone all showed a decreasing trend, and the water content of each type was the highest in setting zone, followed by interference zone, and the lowest in concentration zone, indicating that with the progress of settlement, the active water content in tailings reaches the concentration zone, which decreases and migrates to more stable water. Fig. 16(a) showed that the peak area of ① peak in the setting zone was the largest, while ② peak and

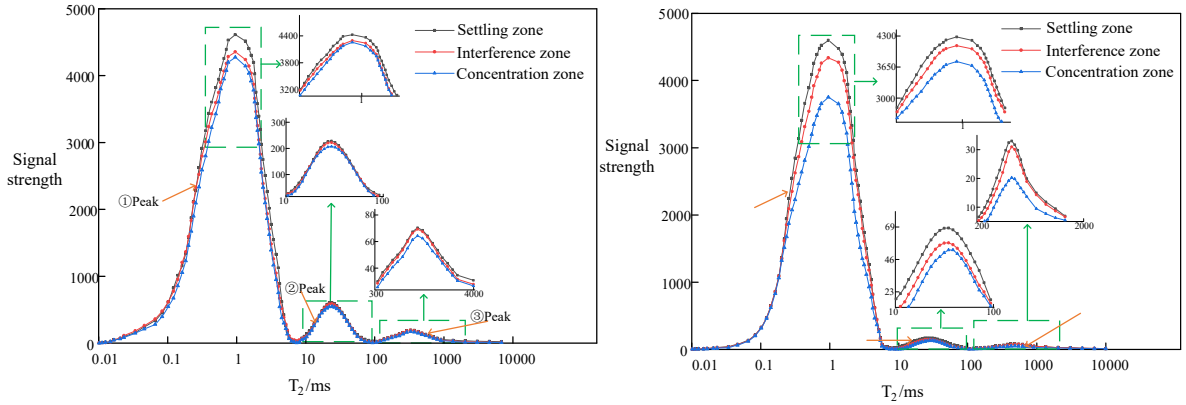

(a) settling for 10min (b) settling for 30min

Fig. 16. Distribution of water T_2 spectra at different sedimentation times in different settlement regions

③ peak were smaller after 10 min of settling. This indicated that the water of the tailings in the setting zone was primarily adsorbed water, followed by pore water content and free water content. In comparison to the setting zone, the peak areas of ① peak, ② peak, and ③ peak in the interference region were decreasing, indicating that the active moisture of tailings is reduced following initial settlement and compression. As shown in Fig. 16(b), the setting zone's ① peak had the biggest peak area, whereas the ② and ③ peaks had lesser areas. This indicated that the water of tailings in the subsidence area is primarily adsorbed water, followed by pore water content and free water content. Peak areas of ① peak, ② peak, and ③ peak in the interference zone and concentration zone were further reduced. Tailings sand was settled and compressed for a long time, and active moisture was greatly reduced. This promoted the transformation of free water into more stable pore water in flocs. To summarize, the areas of the three peaks of tailings sand decreased as it settled for 10 min to 30 min. The water in tailings sand was turned into stable water during settlement, and the water content varies throughout three areas: setting zone, interference zone, and concentration zone. The concentration area had the lowest water content and was also the most stable.

When tailings were settled, the relaxation peak areas of the T_2 spectrum in three areas were investigated. Table 4 exhibited results.

Table 4. Relaxation peak area of tailing T_2 spectrum in three different regions

Setting zone	①Peak		②Peak		③Peak	
	Setting 10min	Setting 30min	Setting 10min	Setting 30min	Setting 10min	Setting 30min
Settling zone	37.41	35.35	1.62	1.11	0.76	0.33
Interference zone	32.98	31.58	1.37	0.82	0.59	0.20
Concentration one	30.01	27.12	1.08	0.53	0.42	0.08

After 10 min of settling, ① peak was measured to be 37.41, ② peak was 1.62, and ③ peak was 0.76 in the setting zone. In the interference zone, ① peak was measured to be 32.98, ② peak was 1.37, and ③ peak was 0.59. The measurements of the ①, ②, and ③ peaks in the concentration zone were 30.01, 1.08, and 0.42, respectively. The area of peak ① was 35.35, ② peak was 1.11, and ③ peak was 0.33 in the setting zone after 30 minutes of settling. In the interference zone, ① peak was 31.58, ② peak was 0.82, and ③ peak was 0.20. In the concentration zone, ① peak was 27.12, ② peak was 0.53, and ③ peak was 0.08. The zone of ① peak in the setting zone, the interference zone, and the concentration zone decreased by 5.51%, 4.24%, and 9.63%, respectively; the ② peak decreased by 31.48%, 40.16%, and 50.93%; and the ③ peak decreased by 56.58%, 66.10%, and 80.95%, respectively. After 30 min settling time, the total water content, which included free water, adsorbed water, and pore water, was measured to have fallen from 31.51% at 10 min to 27.73%, a reduction of 12.00%.

3.4 Strengthening mechanism

3.4.1. Mechanism of flocculant reinforcement

It was commonly known that adding flocculant can improve the sedimentation of ultrafine iron tailings. The sedimentation performance was significantly improved and the particle size of the tailings floc increased significantly with the addition of flocculant. Therefore, further investigation into the mechanism by which flocculant CF enhances tailings sedimentation was carried out.

3.4.1.1. Floc structure analysis

A scanning electron microscope was used to evaluate the flocculant CF, the flocs combined with the floc, and the created ultrafine iron tailings. The results appeared in Fig. 17.

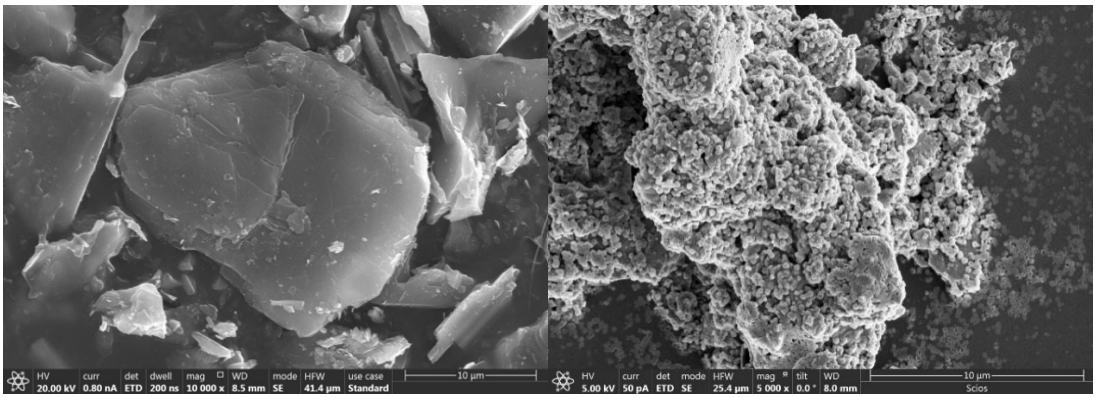

(a) Ultrafine tailings (b) Flocculant CF

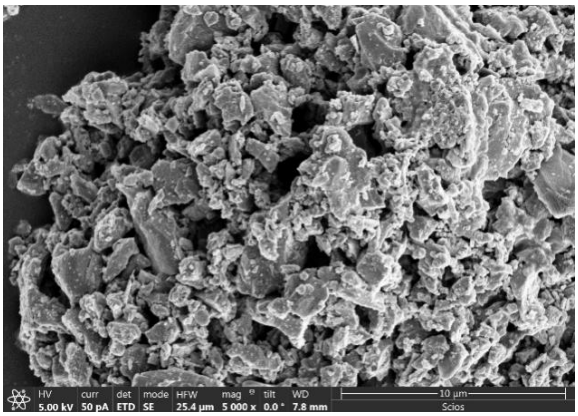

(c) Flocculation after adding flocculant

Fig. 17. Scanning electron microscope images of flocs

The ultrafine iron tailings were found to have generally flat surfaces, prominent and smooth grain edges, and an irregular form, as illustrated in Fig. 17. Spherical particles known as flocculant CF interacted to create a dense structure. It was observed that the polymer flocculant and superfine iron tailings combined to form a compact floc network structure upon the addition of flocculant CF. This finding suggested that flocculant CF had a strong bridging effect that was adsorptive. It was discovered that different sections of these polymer flocculants adhered to tailings particles, and the longer chains increased the sites of contact with the particles. As a result, more particles were able to be adsorbed, which sped up the sedimentation process by forming flocs with long particle sizes, high densities, and compact structures.

3.4.1.2. Analysis of the infrared spectrum

Fourier transform infrared spectroscopy was used to investigate the ultra-fine iron tailings, flocculant, flocculant CF, and flocs supplemented with flocculant. The results were displayed in Fig. 18.

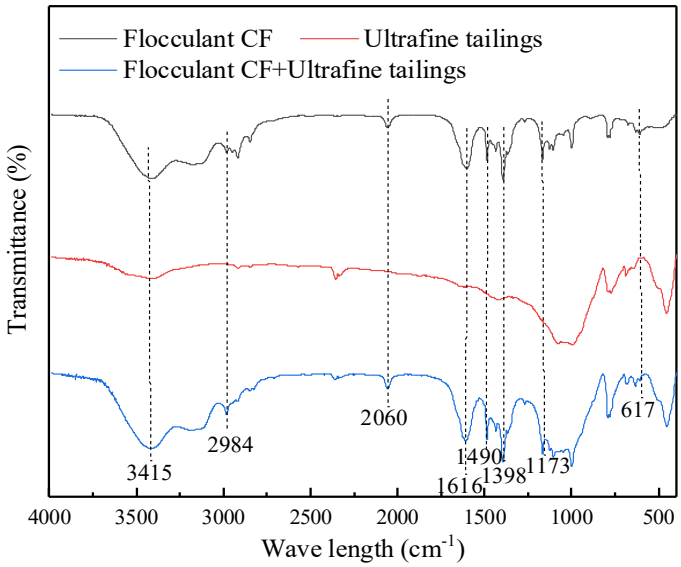

Fig. 18. Fourier transform infrared spectrum

Fig. 18 clearly showed the locations of the absorption peaks for flocculant CF, which were 3415 cm^{-1}, 2984 cm^{-1}, 2060 cm^{-1}, 1616 cm^{-1}, 1490 cm^{-1}, 1398 cm^{-1}, 1173 cm^{-1}, and 617 cm^{-1}. The stretching vibration peaks of hydroxyl groups were responsible for the strong absorption peaks at 3415 cm^{-1} and 2984 cm^{-1}. The wide absorption peaks formed by the superposition of Fe-OH, Al-OH, and coordination water H-OH indicate that flocculant CF contains a large number of hydroxyl groups, with Fe and Al being primarily bonded together by hydroxyl groups. The coordinated water molecules and -OH groups linked to Fe and Al ions were detected by the absorption peak at 2060 cm^{-1}. The stretching vibration of Al-OH-Al was identified as the absorption band between 1616 and 1398 cm^{-1}, the stretching vibration of Fe-OH-Fe was identified as the peak at 1173 cm^{-1}, and the bending vibration of metal hydroxyl groups on the molecular surface was identified as the peak at 617 cm^{-1}. These findings revealed that the flocculant CF sample contained both aluminum and iron polymers that were linked together by hydroxyl groups, and both aluminum and iron in the product are polymerized (Meng et al., 2022; Zou et al., 2022). Fig. 18 observations showed that the addition of flocculant CF significantly changed the spectral bands of iron tailings. Approximately 3415 cm^{-1}, 2984 cm^{-1}, 2060 cm^{-1}, 1616 cm^{-1}, 1490 cm^{-1}, 1398 cm^{-1}, 1173 cm^{-1}, and 617 cm^{-1} were identified as the spectral bands associated with flocculant CF. As a result, it was assumed that the flocculant CF was adsorbed onto the tailings of iron. Strong intra- or intermolecular hydrogen bonding within flocculant CF was proposed as a means of improving flocculation efficiency and, consequently, tailings settling efficiency.

3.4.1.3. Analysis of zeta potential

The zeta potential, a critical parameter for characterizing the stability of a dispersion system, was used to evaluate the repulsive and attractive interactions between the particles in the solution. The addition of flocculant caused a considerable shift in the zeta potential on the surface of the pulp's ultrafine iron tailings particles. The findings of an experiment into how the addition of flocculant CF affected the zeta potential on the tailings particle surface were displayed in Fig. 19.

Tailings sand had a zeta potential of -18.7 mV before flocculant CF was added, as seen in Fig. 19, which indicates that the particles were negatively charged. The absolute value of the zeta potential on the surface of the tailings sand particle reduced quickly when flocculant CF was added, but it then stabilized as the flocculant dosage was raised. According to this observation, flocculant CF, which mainly acts through adsorption and electric neutralization in the flocculation and settlement processes of tailings sand, upsets the stability of the tailings mortar system. The zeta potential was found to drop quickly and approach the zero potential point when the flocculant CF dosage was less than or equal to 120 mg/L. As a result, there was less of the phenomenon known as like-charge repulsion among ore particles. This caused the ore particles to aggregate into floc sediments, which further increased the pace

of sedimentation. The zeta potential was observed to remain largely stable when flocculant CF was added in dosages higher than 120 mg/L. Zeta potential consistency suggested that 120 mg/L had been determined to be the ideal dosage. The largest flocs and best settling performance of the tailings sand particles were produced at this dosage, when the flocculant's ability to promote flocculation reached its peak. Consequently, it was observed that upon dissolution in water, flocculant CF augmented the charge density of Fe^{3+} and Al^{3+} within the solution. The flocculant molecules, possessing lengthy chains with positive active groups, facilitated electric neutralization with the negatively charged tailings particles. The flocculation and sedimentation effectiveness of the tailings particles was further strengthened by this improvement in neutralization.

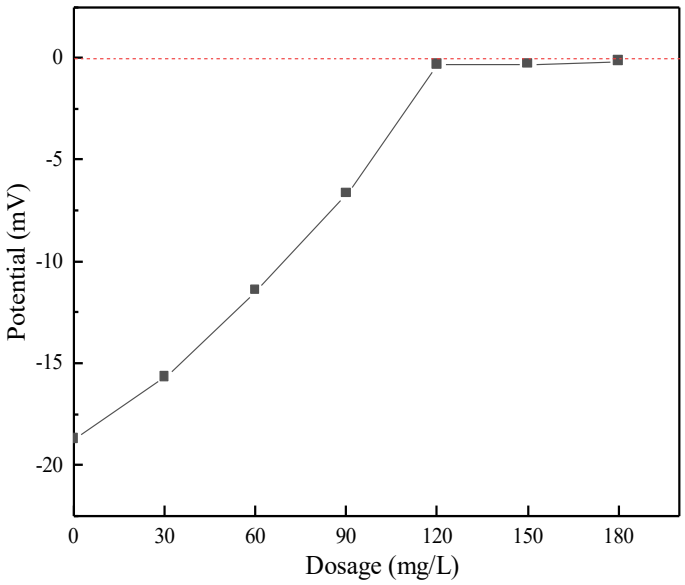

Fig. 19. Zeta potential on the surface of tailings particles

3.4.2. Structural strengthening mechanism

Four components were developed for a new type of deep cone thickener: a small cylinder, a tiny cone, a large cylinder, and a giant cylinder. A variable-sloped cone was added into this thickener. The first big cone had an angle of sixty degrees, while the second little cone had an angle of forty-five degrees. A conical inclined plate was used to guarantee that the clear water area remained at a specific height and to improve the settling time. This successfully expanded the settling area and reduced the ore particles' settling distance. At the same time, a higher secondary sedimentation tank was created to give the depth of the compressed layer required for the manufacturing of high-concentration pulp and to attain a higher concentration underflow (Chen et al., 2022). Two cross-shaped rake frames were mounted on a vertical shaft in the middle of the thickening, and scraper plates were placed underneath the rake frames. Using a feeding mechanism, the thickening's functioning involved introducing the diluted slurry that needed concentration from the upper section of the tank body into the thickener, where it precipitated. After that, the concentrated slurry that had precipitated was removed as an underflow from the tank body's bottom drain, and the clarified water was permitted to overflow from the tank body's upper rim (Olcay et al.,2024). A series of operations, including continuous feeding, underflow discharge, and overflow, defined the thickener's continuous operation. The feed went through a settling process inside the tank after entering the tank body. When the concentration was very thin, the particles first settled freely through a suspension settlement area. The concentration then gradually rose in order to aid in the settling of interference. After passing through a transition area, the particles arrived at the concentration area, which had a noticeably high pulp concentration. As a result, four unique zones were identified in the deep cone thickener, which are listed from top to bottom as the clear setting zone, interference zone, transition zone, and concentration zone (Li and Van, 2023).

The coarser ore particles sank at the bottom of the thickener first, while the finer particles produced a turbid liquid during the settling of suspensions containing tailings particles of different sizes. An

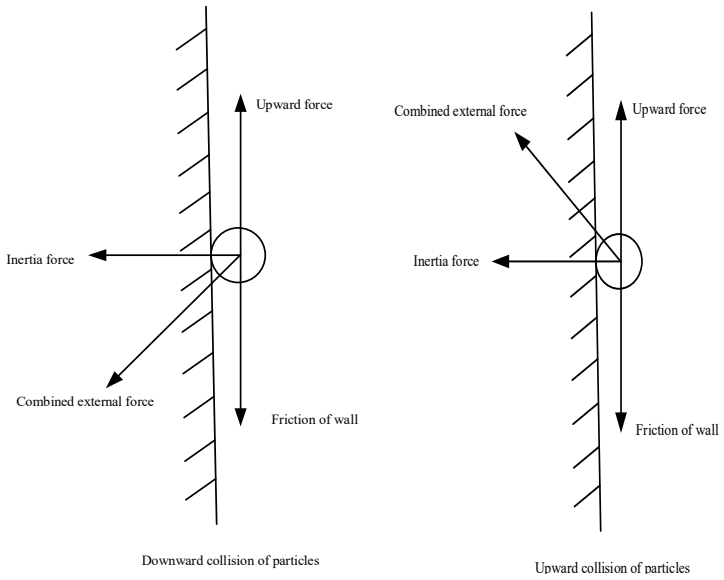

Fig. 20. Collision between particles and container wall

examination of the tailings particles' effects inside the thickener showed that buoyant force, wall friction,inertial force, and a combined force were the main factors affecting the particles inside the container. The particles were directed downward and settled in the concentration area when a significant combined force was applied to them, as demonstrated in Fig. 20. On the other hand, when the combined force was small, it drove the particles upward, which caused the fine tailings particles to create turbid liquid and the settling velocity to drop (Jiao et al., 2021; Li et al., 2022). The addition of flocculant caused the tailings particles to flocculate, which made it easier for the smaller ore particles to settle after the bigger ore particles co-settled. Consequently, the amount of transparent liquid in the uppermost layer increased progressively, and the pulp within the container started to exhibit stratification over time. The setting zone, the transition zone, the interference zone, and the concentration zone were the four distinct zones that were separated from top to bottom in this stratification (Jiao et al., 2022). The majority of the particles in the thickener moved downward, first via the transition zone, then the interference zone, and ultimately into the compression zone. The pulp's solid particles gradually descended to the concentration tank's bottom. Subsequently, they were scraped into the discharge hopper located at the tank's center by the scraper situated below the rake frame and were evacuated by the sand pump. The circular overflow tank, which was located at the upper part of the tank, funneled out the top layer of clean water. The pulp's solid particles sedimented in the direction of the thickener's base, where they were then removed by the sand pump and scraped off by the scraper located under the rake frame. The pure water from the top layer was released using the circular overflow tank, which is located in the upper part of the tank. The pulp's solid particles slowly accumulated at the thickener's base, where they were then removed by the sand pump and scraped off by the scraper that ran underneath the rake frame. The pure water from the upper layer was routed out through the circular overflow tank positioned in the upper half of the tank.

Because of the interference zone's specific inclination angle, some mineral particles that were added to the thickener from the center were directed from the interference zone into the transition zone, where they eventually settled into the concentration zone. Meanwhile, other mineral particles stayed in the interference zone and continued to contribute to the thickening phenomenon. The particles were first concentrated inside the interference zone during this phase.

A coordinate system, shown in Fig. 21, was developed in order to more precisely define the movement process of tailings particles on the inclined plane of the interference zone. The diameter of the tailings particle was denoted as R0, the included angle between the inclined plane and the horizontal plane as α, and the velocity of the water flow falling straight down was u_0. Two components of the water flow velocity were identified: u_1, which ran parallel to the inclined plane, and u_2, which ran perpendicular to it. The downward direction parallel to the inclined plane was found to be the positive direction of the X-axis, and the origin was defined as the point at which the tailings particles met the

inclined plane during their descent. Throughout the settling process, tailings particles continued to accumulate on the slanted surface, which promoted primary thickening. The particles moved from the interference zone to the transition zone when they were affected by the scraper. The transition zone's elevated location gave the particles enough time to settle before they were compressed and concentrated in the concentration zone, which produced the fine tailings particle settling and concentration.

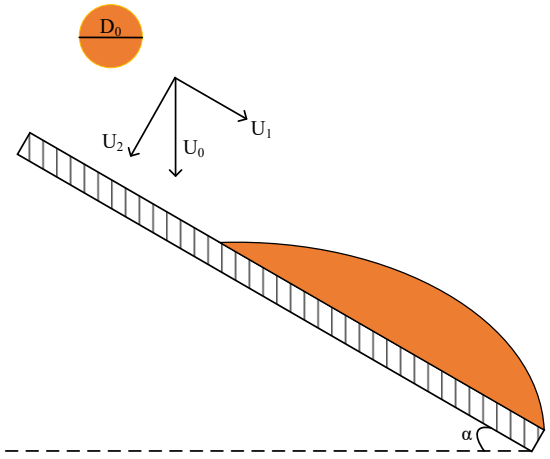

Fig. 21. Coordinate model diagram of particles in the oblique plane of the interference region

4. Conclusions

(1) When the slurry concentration was 4.5%, the feeding speed was 400 mL/min and the rotating speed of scraper was 5 rpm, the underflow concentration was 70.53% when settling for 30 min, and the settling and concentration performance was the best.

(2) Through the electric double layer and adsorption bridging effect, the addition of flocculant CF during the strengthening process resulted in the development of flocs with bigger particle sizes and more compact structures. This made it easier for the flocs to transform free water into pore water that was more stable. After the flocculant was added, the total moisture content, which includes free water, adsorbed water, and pore water, was seen to decrease by 8.43%, from 34.65% to 31.73% in the flocculant-free condition.

(3) In the process of structural strengthening, a new type of deep cone concentrator was used. When the tailings sand settled for 30 min, the total moisture content of the tailings sand decreased from 31.51% at 10 minutes to 27.73%.

Acknowledgments

This work is financially supported by the Doctoral Research Start-up Fund of Guizhou Industry Polytechnic College (2025-rc-04), Interface adsorption desorption effect and regulation mechanism of clay minerals in flocculation flotation process (52374265), Basic research on flotation separation of fine-grained minerals based on asynchronous targeted flocculation regulation(236Z4106G).

References

AHMAD, A.,VAN GENUCHTEN, CM., 2024. *Deep-dive into iron-based co-precipitation of arsenic: A review of mechanisms derived from synchrotron techniques and implications for groundwater treatment*. Water Research.249, 1-8.

CHEN, XM., ZHANG, JL., JIAO, HZ., HU, KJ., WAN, LH., RUAN, ZE., YANG, LH., 2022. *The interactions between Al (III) and Ti (IV) in the composite coagulant polyaluminum-titanium chloride*. Separation and Purification Technology. 282, 1-9.

DENG, NP., FENG, XF., JIN, YB., PENG, ZZ., FENG, Y., TIAN, Y., LIU, Y., GAO, L., KANG, WM., CHENG, BW.,2024. *Design, preparation, application of advanced array structured materials and their action mechanism analyses for high performance lithium-sulfur batteries*. Journal of Energy Chemistry. 89, 266-303.

GAO, X., ZHANG, JH., PEI, DF., WANG, QF., 2019. *Tailings static flocculation sedimentation test in Sanshandao Gold*

Mine. Nonferrous Metals (Mining Section). 71, 116-120.

GUO, GZ., ZHOU, ST., CHEN, YJ., QIN, Y., HUANG, X., LI, YY., 2024. *Enhanced methanogenic degradation and membrane fouling associated with protein-EPS by extending sludge retention time in a high-solid anaerobic membrane bioreactor treating concentrated organic sludge*. Water Research. 248, 1-8.

HAN, CC., TAN, YY., YU, X., 2022. *Flocculation and Settlement Characteristics of Ultrafine Tailings and Microscopic Characteristics of Flocs*. Minerals. 12, 1-15.

HO, QN., FETTWEIS, M., SPENCER, KL., LEE, BJ., 2022. *Flocculation with heterogeneous composition in water environments: A review*. Water Research. 213, 1-6.

JIAO, HZ., CHEN, WL., WU, AX., YU, Y., RUAN, ZE., HONAKER, R., CHEN, XM., YU, JX., 2022. *Flocculated unclassified tailings settling efficiency improvement by particle collision optimization in the feedwell*. International Journal of Minerals, Metallurgy and Materials. 29, 2126-2135.

JIAO, HZ., WU, YC., WANG, W., CHEN, XM., WANG, YF., LIU, JH., FENG, WT., 2021. *Enhanced iron recovery from magnetic separation of ultrafine specularite through polymer-bridging flocculation: A study of flocculation performance and mechanism*. Separation and Purification Technology. 9, 637-650.

KUNDU, T., DASH, N., ANGADI, SI., 2023. *Separation behavior of Falcon concentrator for the recovery of ultrafine scheelite particles from the gold mine tailing*. Separation and Purification Technology. 309, 1-5.

LANDMAN, KA., WHITE, LR., BUSCALL, R., 1988. *The continuous-flow gravity thickener: Steady state behavior*. Aiche Journal. 34, 239-252.

LI, S., WANG, XM., 2016. *Fly-ash-based magnetic coagulant for rapid sedimentation of electronegative slimes and ultrafine tailings*. Powder Technology. 303, 20-26.

LI, WB., CHENG, SK., ZHOU, LB., HAN, YX., 2022. *Enhanced iron recovery from magnetic separation of ultrafine specularite through polymer-bridging flocculation: A study of flocculation performance and mechan*. Separation and Purification Technology. 308, 1-8.

LI, Y., VAN ZD., 2023. *Study on segregation-impacted hindered settling of fine copper tailings using a modified Kynch's approac*. Minerals Engineering. 206, 1-7.

LIU, BB., GAO, BY., GUO, KY., PAN, JW., YUE, QY., 2022. *The interactions between Al (III) and Ti (IV) in the composite coagulant polyaluminum-titanium chloride*. Separation and Purification Technology. 282, 1-9.

MENG, XS., JIANG, M., LIN, SY., GAO, ZY., HAN, HS., WANG, L., ZHANG, CY., LIU, RH., BAO, HJ., JING, GG., SUN, W., 2022. *Metal ions synergize with gangue minerals to remove residual sodium oleate from mineral processing wastewater*. Journal of Cleaner Production. 388, 1-12.

OLCAY, RH ., VALADAO, GE., ARAUJO, AC., REYES, IA., FLORES, MU., 2024. *Dewatering of Fine Tailings for Disposal in Dams Using a Column Thickener, Deep Cone Classifier, and Hyperbaric Filtration*. Mining Metallurgy & Exploration. 41, 335-344.

PENG, NB., WU, AX., WANG, HJ., SUN W., CHEN H., 2015. *Research on Flocculation Sedimentation Technology of Unclassified-tailings*. Mining Research and Development. 35, 35-38.

TAN, W., 2020. *Experimental study on deep cone thickening of ultrafine unclassified tailings*. Nonferrous Metals (Mining Section). 72, 102-105.

TANG, CM., GUO, ZQ., PAN, J., ZHU, DQ., LI, SW., YANG, CC., TIAN, HY., 2023. *Current situation of carbon emissions and countermeasures in China's ironmaking industry*. International Journal of Minerals, Metallurgy and Materials. 30, 1633-1650.

WEN, S., 2024. *Thermodynamic theory of flotation for a complex multiphase solid–liquid system and high-entropy flotation. International Journal of Minerals*. Metallurgy and Materials. 31, 1177-1197.

YAO, MY., HAO, LM., XU, B., JIANG, JG., ZHANG, W., 2023. *Analysis of Influence of Tailings Concentration and Discharge Technology on Safe Operation of Tailings Pond*. Modern Mining. 39, 201-204.

ZHANG, LF., WANG, HJ., WU, AX., YANG, K., ZHANG, X., GUO, JB., *Effect of flocculant dosage on the settling properties and underflow concentration of thickener for flocculated tailing suspensions*. Water Science & Technology. 88, 304-320.

ZHANG, YQ., DING, SH., SI, WH., YIN, QL., YANG, CYM., SHI, WQ., XING, YW., GUI, XH., 2024. *Effect of Particle Size and Hydrophobicity on Bubble-Particle Collision Detachment at the Slurry–Foam Phase Interface*. ACS Omega. 9, 4966-4973.

ZOU, Y., LIU, Q., LIU, WJ., 2022. *Study on the Relation between Tailing Particle Size and Tailing Slurry Underflow Concentration*. Advances in Civil Engineering. 2022. 1-8.